

## Diffraction from domain-wall systems

Peter Zeppenfeld, Klaus Kern, Rudolf David, and George Comsa

*Institut für Grenzflächenforschung und Vakuumphysik, Kernforschungsanlage Jülich, 5170 Jülich, West Germany*

(Received 9 February 1988)

We present kinematical calculations of the diffraction patterns from domain-wall systems on a hexagonal substrate lattice. Diffraction-peak positions and intensities are calculated for the  $(\sqrt{3} \times \sqrt{3})R30^\circ$  commensurate-to-incommensurate phase transition, assuming all possible domain-wall systems: heavy, superheavy, light, and superlight walls for both the hexagonal and the striped symmetry. In addition, we allow for wall relaxation and determine its effect on the diffraction-peak intensities. As an example, the  $(\sqrt{3} \times \sqrt{3})R30^\circ$  commensurate-to-incommensurate phase transition of Xe/Pt(111) is explained as a continuous transition involving striped superheavy walls with increasing relaxation followed by a first-order transition into a hexagonal incommensurate phase.

### INTRODUCTION

Considerable interest has been given in the last decade to the commensurate- (*C*-) incommensurate (*I*) phase transition in two-dimensional systems. In theoretical<sup>1,2</sup> as well as experimental<sup>3,4</sup> investigations the *C-I* phase transition is described in terms of domain-wall formation: At the transition, commensurate areas start to be separated by regions of different density. These regions are called walls. Their density is higher or lower than that of the commensurate areas depending on whether the *I* phase has a higher or a lower density, respectively. Proceeding further in the transition the number of walls increases (i.e., their mutual mean distance decreases) at the expense of the commensurate domains, and eventually the incommensurate walls form a homogeneous *I* phase.

The number of topologically different, possible domain-wall systems is determined by the order of commensurability of the overlayer,<sup>5</sup> i.e., the number of equivalent types of adsorption sites in the commensurate phase. In the case of a  $(\sqrt{3} \times \sqrt{3})R30^\circ$  overlayer the order of commensurability is  $p=3$ . The corresponding  $p-1=2$  domain-wall systems are called heavy and superheavy<sup>6</sup> if the *I* phase has a higher density than the *C* phase and light and superlight if it has a lower density.<sup>4</sup> Depending on the wall crossing energy  $\Lambda$ , the walls may either form a striped pattern or may cross each other yielding a honeycomb-type array of walls (often called hexagonal).<sup>7</sup> If  $\Lambda > 0$ , wall crossings are energetically unfavorable and consequently a striped domain-wall system is formed. Instead,  $\Lambda < 0$  results in the honeycomblike domain-wall system. A survey of all possible domain-wall systems is given in Fig. 1.

To investigate domain-wall system, the most commonly used method is to measure the diffraction of x rays,<sup>3,4</sup> low-energy electrons (LEED) (Ref. 8), or thermal He atoms.<sup>9</sup> Therefore information on the type of domain-wall structure has to be extracted from the diffraction-peak positions and intensities. The question arises as to if and how a domain-wall system can unambiguously be identified and characterized by analyzing the diffraction

pattern.

Following other authors,<sup>3</sup> who calculated the structure factor within the kinematical approximation for several hexagonal domain-wall systems, we give here a complete description of the diffraction-peak positions and intensities for all possible domain-wall systems occurring in a  $(\sqrt{3} \times \sqrt{3})R30^\circ$ -*I* phase transition. We then allow the walls to relax (i.e., the shift between two neighboring commensurate domains is distributed over a characteristic number  $\lambda$  of atoms in the boundary region, which is then called the width of the wall).

We show that the relaxation changes the diffraction-peak intensities but not their position. From the position of the diffraction peaks we can unequivocally extract the type of domain-wall structure and their symmetry (striped in a definite symmetry direction or hexagonal). From the relative intensities we can estimate the degree of wall relaxation.

As an example we apply our results to the high-resolution He-atom diffraction data<sup>9</sup> from the  $(\sqrt{3} \times \sqrt{3})R30^\circ$ -*I* phase transition of Xe physisorbed on the Pt(111) surface.

### NUMERICAL RESULTS

The structure factor  $S(\mathbf{Q})$ , where  $\mathbf{Q}=(Q_x, Q_y)$  denotes the scattering wave vector parallel to the surface, is calculated using the kinematical approximation:

$$S(\mathbf{Q}) = \sum_{k=0}^M f_k \exp(-i\mathbf{Q} \cdot \mathbf{r}_k) \quad (1)$$

where  $M$  is the number of scattering atoms, and  $\mathbf{r}_k$  and  $f_k$  the position and atomic form factor of atom  $k$ , respectively. Since we are dealing with only one kind of atom in the first layer, we can take  $f_k=1$  in (1). The normalized scattered intensity is then simply given by

$$I(\mathbf{Q}) = \frac{1}{M^2} \left| \sum_{k=0}^M \exp(-i\mathbf{Q} \cdot \mathbf{r}_k) \right|^2. \quad (2)$$

Assuming periodic boundary conditions, the number of scattering atoms  $M$  can be reduced to fit into a unit cell

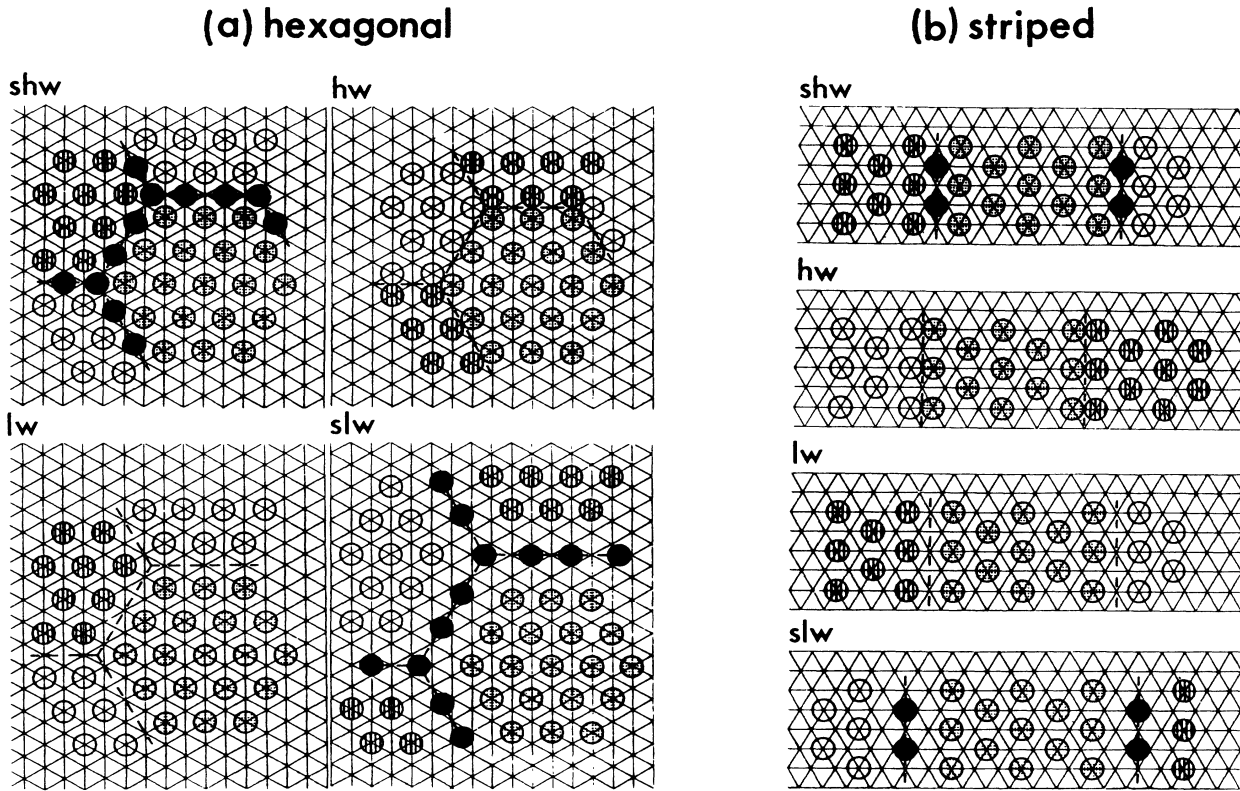


FIG. 1. Domain-wall systems for a  $(\sqrt{3} \times \sqrt{3})R30^\circ$  phase on a hexagonal substrate lattice. (a) hexagonal symmetry, (b) striped symmetry. Different shadowing is used to indicate the three topologically different adsorption sites. Abbreviations used throughout: shw, superheavy; hw, heavy; lw, light; and slw, superlight wall system.

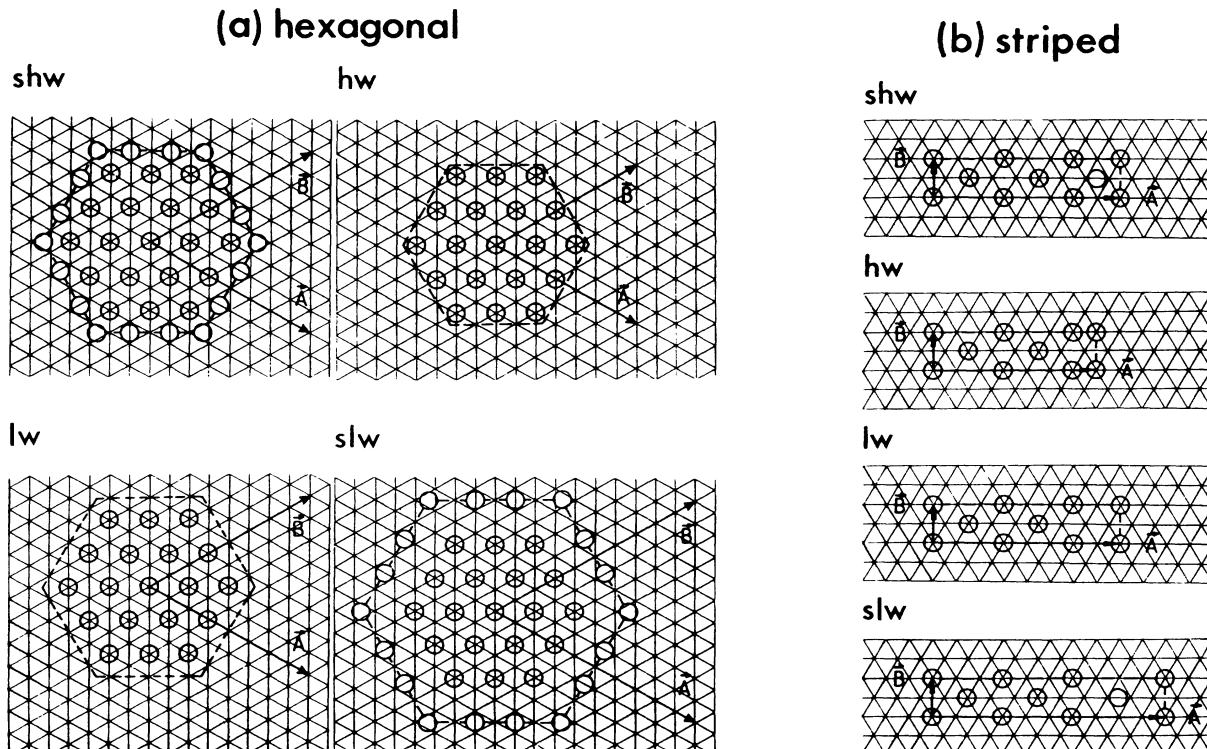


FIG. 2. Unit cells used to calculate the structure factor for the unrelaxed domain-wall system as illustrated in Fig. 1; (a) hexagonal symmetry, (b) striped symmetry. The number of atomic rows  $N=6$ ;  $l = |\mathbf{A}|$  is the domain length.

defined by a set of two vectors  $\mathbf{A}$  and  $\mathbf{B}$  which is then reproduced by every superlattice vector  $\mathbf{R} = j_1 \mathbf{A} + j_2 \mathbf{B}$ ;  $j_1, j_2 \in \mathbb{Z}$ . The shape of the unit cell and the distribution of the atoms within the unit cell is defined by the type of the domain-wall system,<sup>10</sup> as shown in Fig. 2. The domain-wall systems will be discussed first by assuming no relaxation of the atom positions: the walls accordingly consist of the one-dimensional boundary line separating two neighboring  $(\sqrt{3} \times \sqrt{3})R 30^\circ$  commensurate domains. A large unit cell gives rise to a large number of diffraction spots (at  $\mathbf{Q}$  values for which  $\mathbf{RQ} = 2\pi n$ ,  $n \in \mathbb{Z}$ ). The relative intensities of the diffraction spots are determined by the position of the atoms within the unit cell. The calculation shows that only a few reciprocal superlattice points close to the commensurate lattice spots in  $\mathbf{Q}$  space have noticeable intensity (this may be rationalized by the fact that most of the atoms in the unit cell still occupy commensurate lattice sites).

In Fig. 3 we indicate all spots with intensities  $I(\mathbf{Q}) > 0.05$  for the different kind of domain-wall systems (the spot area in Fig. 3 is a measure of the relative intensity). The calculation has been performed assuming a

domain length of  $N=20$  atomic rows. All diffraction-spot positions are given relative to the original commensurate lattice spots in units of  $\epsilon$  defined by  $\epsilon = 4\pi/3l$ , where  $l = |\mathbf{A}|$  is the length of the domain. In the following we give a brief discussion of the results.

As a main feature, all the domain-wall systems yield in the  $\Gamma\bar{M}$  direction a triplet diffraction-spot pattern<sup>11</sup> in the vicinity of the (1,1) and (2,2) commensurate diffraction spots indexed by the subscript  $c$  in Fig. 3. The relative position of the two off-axis peaks and the single on-axis peak depends on the kind of domain-wall system; it changes in a characteristic way when moving from the first-order (1,1) to the second-order (2,2) commensurate diffraction spot. As can be seen from Fig. 3, in the case of striped symmetry, there are two intercalated triplet patterns, the inner one having much higher intensity. Note that the inner spots of this high-intensity triplet are at a distance  $\epsilon/2$  from the commensurate position. For the same domain length  $l = |\mathbf{A}|$  this is just half as large as for the case of hexagonal symmetry; i.e., in order to obtain the same splitting, the mean domain length in the striped system has to be a factor of 2 smaller. While the

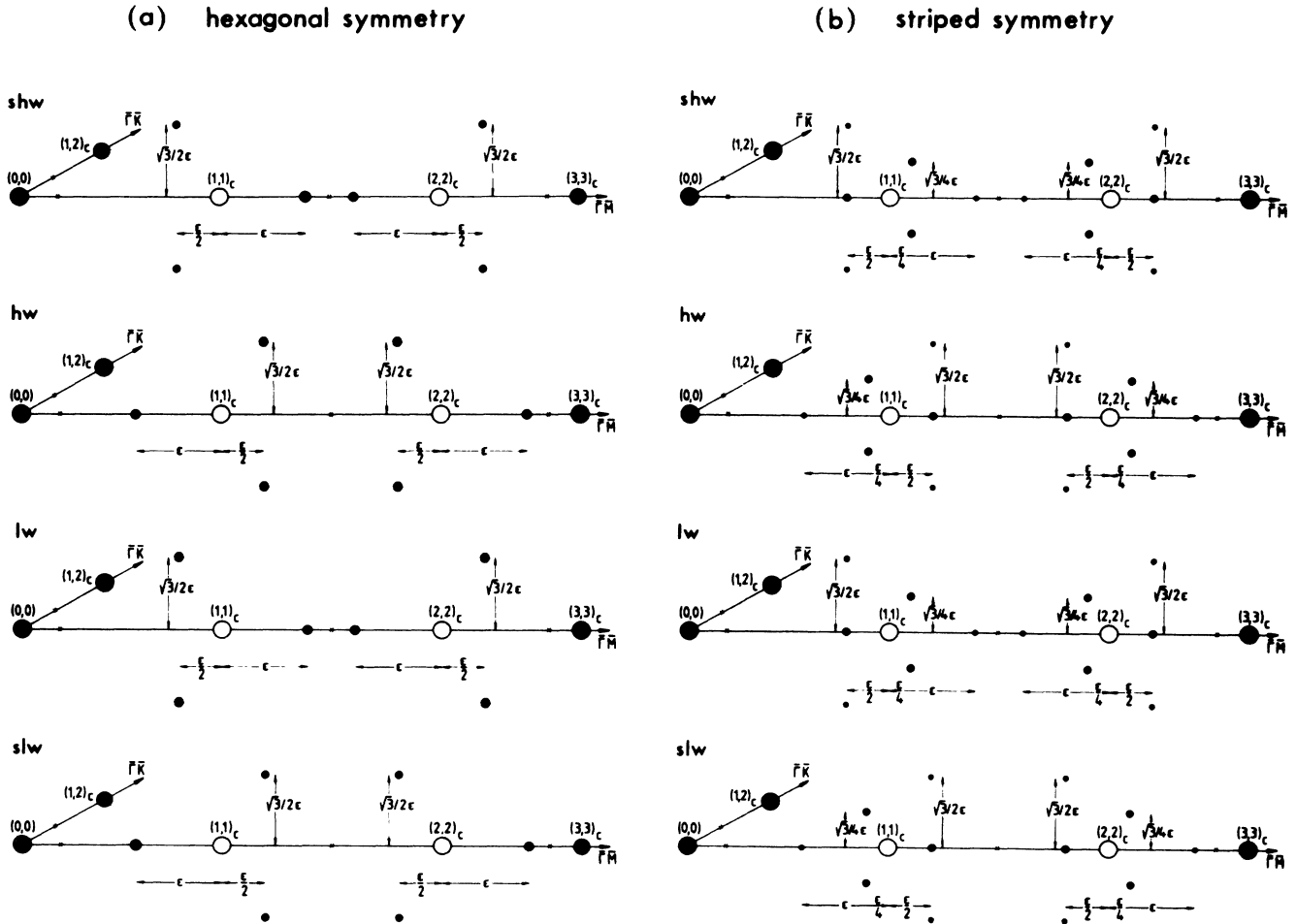


FIG. 3. (a) Calculated diffraction pattern of the domain-wall systems with hexagonal symmetry using the same type of unit cells as in Fig. 2(b) but taking  $N=20$ .  $\epsilon$  is defined by the domain length  $l$ :  $\epsilon = 4\pi/(3l)$ . (b) Same as (a) but for striped symmetry.

first- and second-order diffraction spots in the  $\bar{\Gamma}\bar{M}$  direction split into a triplet spot pattern around the commensurate position, the third-order spot (3,3) for all domain-wall systems does not split and has maximum intensity at the commensurate position. This is not surprising since all domain-wall systems consist of domains shifted by one or by two-thirds of the interatomic row distance, and thus their scattering amplitudes constructively interfere in the third-order diffraction peak.

These shifts between the commensurate domains occur perpendicularly to the walls. All the domain walls described here being along the  $\bar{\Gamma}\bar{K}$  direction (see, e.g., Fig. 1), the diffraction in the  $\bar{\Gamma}\bar{K}$  direction is not influenced by the presence of unrelaxed walls; therefore single diffraction peaks at the original commensurate lattice diffraction spots with maximum intensity as shown in Fig. 3 are to be expected.

We have considered so far only an abrupt phase shift of neighboring commensurate domains, without allowing for a change of the atomic positions within the domains. This is rather unphysical, since the stress induced by a rigid wall will force the nearby atoms to shift towards the wall (in the case of light and superlight walls) or away from it (heavy and superheavy walls). By this relaxation of the atom positions within the domains, the total phase shift between two neighboring commensurate domains is smoothly distributed over a range of interatomic distances. Figure 4 illustrates the relaxation of a superheavy domain-wall system: Fig. 4(a) shows the nonrelaxed case discussed above and Fig. 4(b) a partial relaxation, involving a characteristic wall width  $\lambda$ ; Fig. 4(c) represents the limiting case of a fully relaxed domain-wall system: domain walls and domains are indistinguishable, the

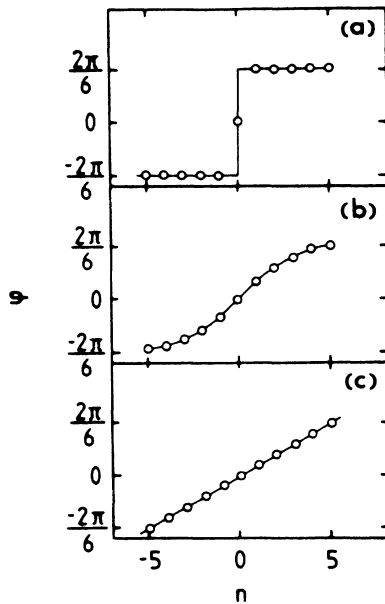


FIG. 4. Relaxation in the superheavy domain-wall system ( $N=10$ ). The phase shift  $\varphi$  is plotted for each atomic row  $n$  ( $n=0$  denotes the wall position). (a) No relaxation, (b) partial relaxation using Eq. (3) with  $\varphi_0=2\pi/3$  and  $\lambda=3$ , (c) fully relaxed, incommensurate phase.

overlayer becomes a uniformly compressed incommensurate phase. The fully relaxed hexagonal domain-wall system is isotropically compressed and therefore leads to single diffraction spots at positions  $Q((n,n)_c)+n\epsilon$  and  $Q((2n,n)_c)+\sqrt{3}n\epsilon$  in the  $\bar{\Gamma}\bar{M}$  and  $\bar{\Gamma}\bar{K}$  directions, respectively [Fig. 5(a)], while in the striped superheavy domain-wall system the compression is uniaxial in the direction perpendicular to the orientation of the walls, yielding diffraction-spot triplets<sup>11</sup> as shown in Fig. 5(b).

It is interesting to see how the diffraction-spot pattern changes by gradually increasing the relaxation from the unrelaxed to the fully relaxed system. Following Ref. 3 we have introduced an algebraic form for the relaxation:

$$\Delta\varphi(n) = \frac{\varphi_0}{2} \tanh\left[\frac{n}{\lambda}\right], \quad n \in \mathbb{Z}. \quad (3)$$

Equation (3) gives the shift of atom  $n$  from its original commensurate position with respect to the wall position ( $n=0$ ). The total shift  $\varphi_0$  between two neighboring domains is now smoothed over a region characterized by the number  $\lambda$  that can be interpreted as the wall thickness in units of the interatomic row distance [the relaxation in Fig. 4(b) is given by Eq. (3) with  $\varphi_0=2\pi/3$  and  $\lambda=3$ ].

In Fig. 6 we show the results of a calculation of the intensities for the diffraction spots in the vicinity of the (2,2) commensurate spot as a function of the wall thickness  $\lambda$  for a superheavy domain-wall system with hexagonal (a) and striped (b) symmetry (the number of interatomic rows was taken to be  $N=20$ ). It can be easily seen in Fig. 6 how the diffraction-spot pattern gradually evolves from the unrelaxed case (Fig. 3) to the fully relaxed case (Fig. 5). By choosing another functional form for the relaxation, the results are only marginally affected. We therefore believe, as long as the kinematical theory is applicable, that the relative intensities of the

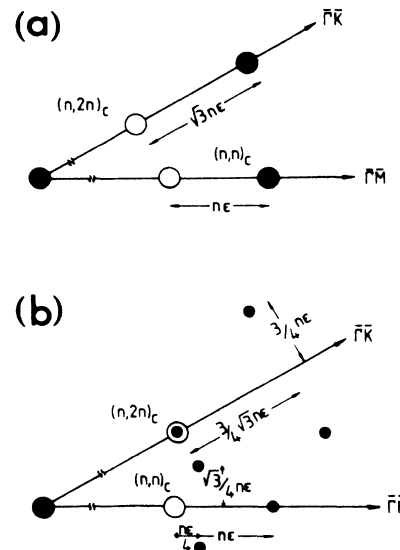


FIG. 5. Diffraction pattern of the fully relaxed hexagonal (a) and striped (b) superheavy domain-wall system.

diffraction spots can give a reasonable estimate of the strength of relaxation.

In most theoretical and experimental studies dealing with structural phase transitions, the adlayers considered are described in terms of the misfit  $m$ , defined as the rela-

tive difference between the commensurate and the incommensurate lattice spacings  $d_C$  and  $d_I$ , respectively; i.e.,  $m = |(d_C - d_I)/d_C|$ . Before applying the results presented above to our experimental data, we therefore establish the connection between the lattice misfit  $m$  and the spot splitting parameter  $\epsilon$  obtained from the diffraction pattern around the commensurate position  $Q((n, n)_c)$ . A straightforward calculation yields  $m = n\epsilon/[Q((n, n)_c) + n\epsilon]$ ,  $m = n\epsilon/[2Q((n, n)_c) + n\epsilon]$ ,  $m = n\epsilon/[Q((n, n)_c) - n\epsilon]$ , and  $m = n\epsilon/[2Q((n, n)_c) - n\epsilon]$ , for superheavy, heavy, superlight, and light walls, respectively. As  $\epsilon$  is generally small, the misfit equals approximately  $n\epsilon/Q((n, n)_c)$  for the superheavy and superlight domain-wall systems and about half this value for the heavy and light domain-wall systems.

It should be pointed out, however, that (a) the misfit  $m$  is properly defined only for the fully relaxed domain-wall systems, i.e., for homogeneous, incommensurate adlayers and (b) the misfit may be different along different directions; indeed, in the direction parallel to the walls of the striped domain-wall systems  $m = 0$ .

#### THE $(\sqrt{3} \times \sqrt{3})R 30^\circ$ -I PHASE TRANSITION OF Xe/Pt(111)

To show how the results obtained above can be used to characterize the  $C$ - $I$  transition, we will apply them to the case of the  $(\sqrt{3} \times \sqrt{3})R 30^\circ$ - $I$  phase transition of Xe/Pt(111). This adsorption system seems to be one of the most interesting representatives of quasi-two-dimensional structural phase transitions.<sup>9,12</sup> Xe on Pt(111) exhibits at least six different phases and corresponding phase transitions in the monolayer regime, all of which can be explained by theory.<sup>7,13</sup> In our example we focus on the  $C$ - $I$  transition.

Let us first summarize the main features which have been clearly established so far.<sup>12</sup> The commensurate  $(\sqrt{3} \times \sqrt{3})R 30^\circ$  structure has been found to be stable in an extended coverage ( $\Theta_{Xe} \leq 0.33$ ) and temperature ( $62 \leq T \leq 99$  K) range. Upon increasing the coverage above  $\Theta_{Xe} = 0.33$  (the maximum coverage of a commensurate layer fully covering the substrate) or decreasing the temperature below 62 K the commensurate lattice is destabilized. The ensuing  $C$ - $I$  phase transition has been found to be continuous and at misfits  $> 4\%$  the nature of the incommensurate phase has been unambiguously identified: for misfits between 4% and 6.5% the measured diffraction patterns are consistent with a fully relaxed striped phase, i.e., a uniaxially compressed layer (see Fig. 5): The observed  $(2,2)_{Xe}$  diffraction feature is a triplet structure with an out of plane doublet located at  $Q((2,2)_c) + \epsilon/2$ , symmetrical with respect to the  $\bar{\Gamma}\bar{M}_{Xe}$  direction and with a single on-axis peak at  $Q((2,2)_c) + 2\epsilon$ ; whereas the  $(1,2)_{Xe}$  pattern consists of a peak at the commensurate position and a shallow doublet at  $Q((1,2)_c) + \frac{1}{4}\sqrt{3}\epsilon$  (see Fig. 2 in Ref. 9).

Here we address the question concerning the nature of the striped incommensurate phase close to the  $C$ - $I$  transition, i.e., at smaller misfits, where the topography of the adlayers should be more consistent with a domain-wall phase than with a homogeneous, incommensurate phase.

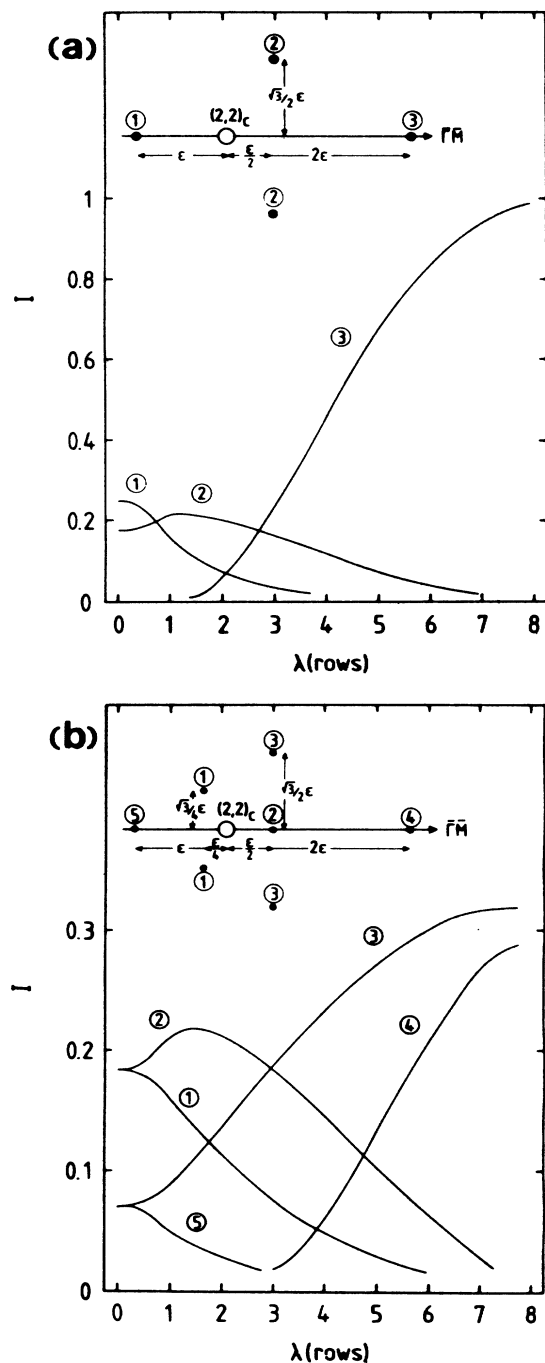


FIG. 6. Diffraction-spot intensities for the superheavy domain-wall systems with hexagonal (a) and striped (b) symmetry in the vicinity of the  $(2,2)$  commensurate diffraction spot with increasing relaxation (wall thickness  $\lambda$ ). The spot positions are indicated in the inset (see also Fig. 3). The number of rows is  $N = 20$  resulting in a misfit  $m = 3.3\%$ .

In particular, we want to infer the type of domain-wall system (heavy or superheavy) as well as the degree of relaxation. They are more difficult to obtain, because at small misfits the characteristic splittings are also small and thus often not clearly resolved.

In Fig. 7 we show *azimuthal* He-diffraction scans of the  $(2,2)_{\text{Xe}}$  diffraction feature, taken from a weakly incommensurate Xe monolayer. The Xe monolayer has been prepared by exposing the Pt(111) crystal at  $T=50$  K to Xe gas until a coverage of  $\Theta_{\text{Xe}} \approx 0.36$  was obtained and then cooling down to 25 K. The diffraction scans have

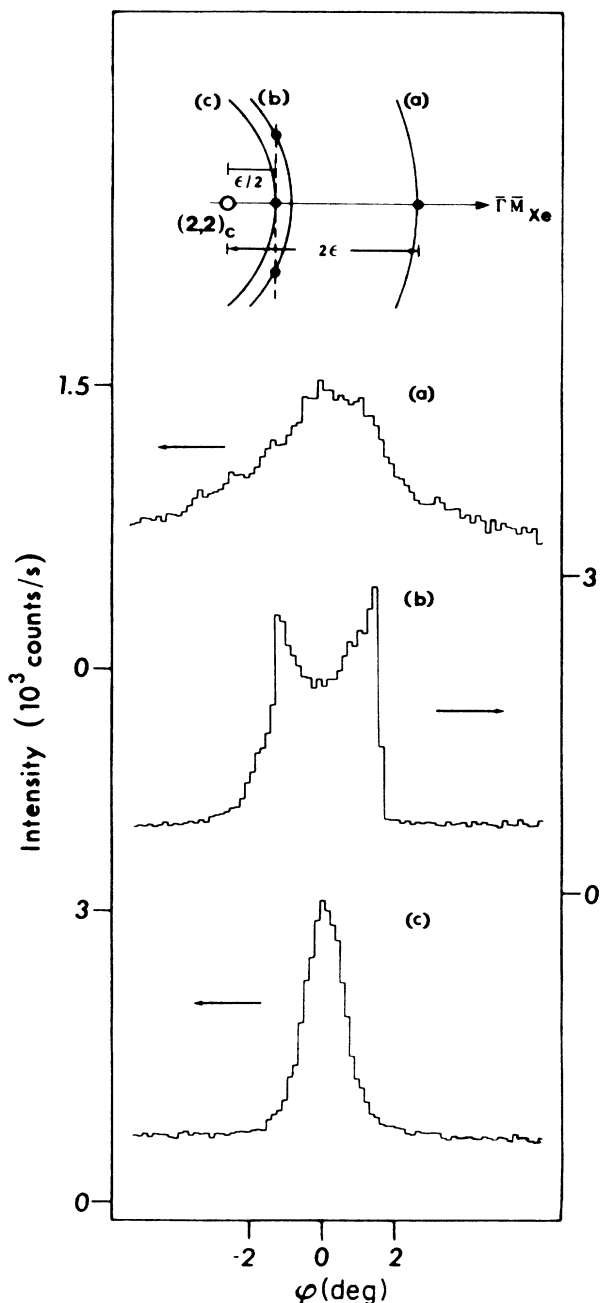


FIG. 7. Azimuthal scans of the  $(2,2)_{\text{Xe}}$  diffraction at various absolute wave-vector transfers: (a)  $Q=3.126 \text{ \AA}^{-1}$ , (b)  $Q=3.047 \text{ \AA}^{-1}$ , and (c)  $Q=3.045 \text{ \AA}^{-1}$ , taken from an incommensurate Xe monolayer on Pt(111) with a misfit of 3.4%.

been recorded with a He beam of wavelength  $\lambda_{\text{He}}=1.062 \text{ \AA}$  and a monochromaticity  $\Delta\lambda_{\text{He}}/\lambda_{\text{He}} \approx 0.007$ . Azimuthal scans are monitored by rotating the crystal around its surface normal; i.e., in each scan, the absolute wave-vector transfer  $Q=|\mathbf{Q}|$  is kept constant, while the wave-vector transfer projected onto the high-symmetry axis of the adlayer (here  $\bar{\Gamma}\bar{M}_{\text{Xe}}$ ) varies as the cosine of the angle between the scattering direction and the symmetry axis. In Fig. 7(a) we show an azimuthal scan taken at  $Q=3.126 \text{ \AA}^{-1}$ . In the case of superheavy walls, the on-axis peak observed corresponds to the  $Q=Q((2,2)_c)+2\epsilon$  peak with  $Q((2,2)_c)=3.020 \text{ \AA}^{-1}$  and  $2\epsilon=0.106 \text{ \AA}^{-1}$  [spot 4 in Fig. 6(b)]; the resulting misfit of the layer is  $2\epsilon/[Q((2,2)_c)+2\epsilon]=3.4\%$ . Scan (b) displays an azimuthal profile taken at  $Q=3.047 \text{ \AA}^{-1}$ . The observed doublet corresponds to the calculated doublet with the projected wave vector  $Q((2,2)_c)+\epsilon/2=3.045 \text{ \AA}^{-1}$  [spot 3 in Fig. 6(b)]. The azimuthal angular separation of the two doublet peaks  $\Delta\varphi \approx 3.1^\circ$  corresponds to an orthogonal wave-vector component of the two peaks at  $0.10 \text{ \AA}^{-1}$  and  $-0.10 \text{ \AA}^{-1}$ , respectively. This is in excellent agreement with the predicted value  $\sqrt{3}\epsilon/2=0.09 \text{ \AA}^{-1}$  using  $\epsilon=0.106 \text{ \AA}^{-1}$  as obtained above. Finally, scan (c) shows an azimuthal profile recorded at a polar angle only  $0.018^\circ$  apart from the polar angle of scan (b), i.e., at an absolute wave vector  $Q=3.045 \text{ \AA}^{-1}$ . We observe a sharp on-axis peak and no doublet [spot 2 in Fig. 6(b)]. Accordingly at misfits of about 3.4%, the second diffraction order features is composed of one single on-axis peak at  $Q((2,2)_c)+2\epsilon$  and three peaks, one on axis and a doublet, all with the same projected wave vector at  $Q((2,2)_c)+\epsilon/2$ . These three peaks could be resolved only because of the particular characteristic of the azimuthal scans, i.e., scans with constant *absolute* wave-vector transfer and not with constant *projected* wave vector.

An energy analysis of the diffracted He intensities in the patterns discussed above proved the purely elastic nature of the scattered intensity; furthermore, the diffraction spot splittings occur in a very narrow  $Q$  range, so that a significant dependence of the scattering form factor on  $Q$  over this range can be discarded. This justifies the use of the kinematically calculated relative intensities to deduce the amount of relaxation.

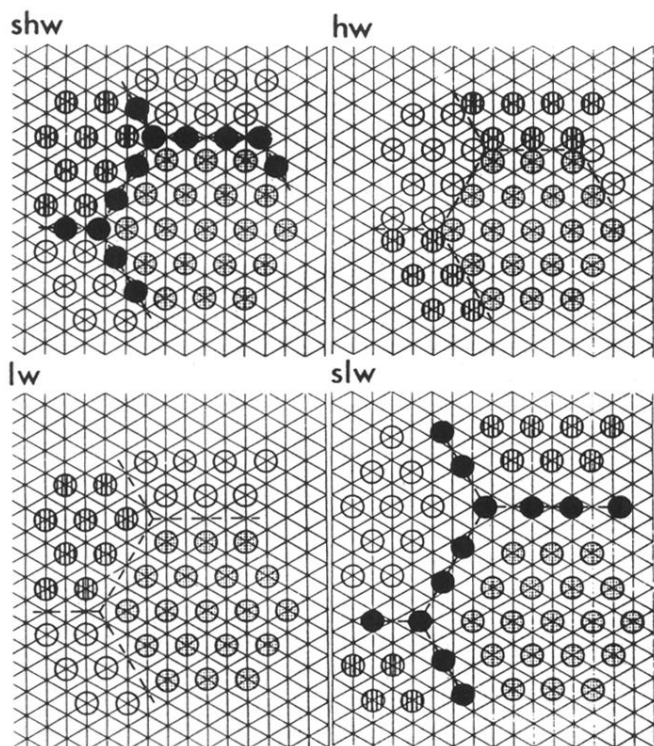
The comparison with Figs. 3 and 6 shows that the incommensurate Xe layer on Pt(111) at a misfit of 3.4% is a *striped phase* involving *superheavy walls* [running in the  $\bar{\Gamma}\bar{K}_{\text{Xe}}$  direction, see Fig. 1(b)]. Comparing the intensities of the various measured diffraction peaks in Fig. 7 with the theoretically evaluated relative intensities as a function of the wall relaxation (Fig. 6, corresponding to a misfit of 3.3%), provides us with an estimate of the width of the superheavy walls of  $\lambda \sim 3\text{--}5$  interatomic rows.

#### SUMMARY

We have shown how a particular domain-wall system involved in a  $(\sqrt{3} \times \sqrt{3})R30^\circ\text{--}I$  transition on a hexagonal substrate lattice can be identified from the spot positions in the diffraction pattern. Within the kinematical approximation we can interpret relative intensities in terms of relaxation of the domain walls.

- <sup>1</sup>J. Villian, in *Ordering in Strongly Fluctuating Condensed Matter Systems*, edited by T. Riste (Plenum, New York, 1980), p. 221.
- <sup>2</sup>P. Bak, *Rep. Prog. Phys.* **45**, 587 (1982).
- <sup>3</sup>P. W. Stephens, P. A. Heiney, R. J. Birgeneau, P. M. Horn, D. E. Moncton, and G. S. Brown, *Phys. Rev. B* **29**, 3512 (1984).
- <sup>4</sup>H. Hong, R. J. Birgeneau, and M. Sutton, *Phys. Rev. B* **33**, 3344 (1986).
- <sup>5</sup>D. A. Huse and M. E. Fisher, *Phys. Rev. Lett.* **49**, 793 (1982).
- <sup>6</sup>M. Kardar and A. N. Berker, *Phys. Rev. Lett.* **48**, 1552 (1982).  
We use the definition of heavy and superheavy walls according to Kardar and Berker. In Ref. 5 heavy walls are called light and superheavy walls heavy.
- <sup>7</sup>P. Bak, D. Mukamel, J. Villain, and K. Wentowska, *Phys. Rev. B* **19**, 1610 (1979).
- <sup>8</sup>A. Q. D. Faisal, M. Hamichi, G. Raynard, and J. A. Venables, *Phys. Rev. B* **34**, 7440 (1986).
- <sup>9</sup>K. Kern, R. David, P. Zeppenfeld, R. L. Palmer, and G. Comsa, *Solid State Commun.* **62**, 391 (1987).
- <sup>10</sup>M. Nielsen, J. Als-Nielsen, and J. P. McTague, in *Ordering in Two Dimensions*, edited by S. K. Sinha (North-Holland, Amsterdam, 1980), p. 135.
- <sup>11</sup>Since there are three equivalent, nondegenerated orientations for the stripped domain-wall system, the diffraction pattern is obtained by summing up the contribution of each with equal probability  $\frac{1}{3}$ .
- <sup>12</sup>K. Kern, P. Zeppenfeld, R. David, R. L. Palmer, and G. Comsa, in *Structure of Solid Surfaces II*, edited by J. F. van der Veen and M. A. van Hove (Springer, Heidelberg, 1988), p. 488.
- <sup>13</sup>K. Kern, *Phys. Rev. B* **35**, 8265 (1987).

(a) hexagonal



(b) striped

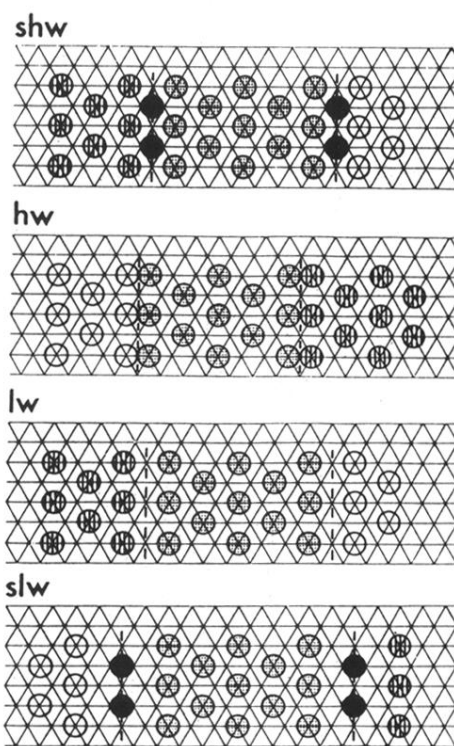


FIG. 1. Domain-wall systems for a  $(\sqrt{3} \times \sqrt{3})R 30^\circ$  phase on a hexagonal substrate lattice. (a) hexagonal symmetry, (b) striped symmetry. Different shadowing is used to indicate the three topologically different adsorption sites. Abbreviations used throughout: shw, superheavy; hw, heavy; lw, light; and slw, superlight wall system.